Near-Infrared Coronagraphy of the GG Tauri A Binary System

Itoh, Yoichi ; Tamura, Motohide ; Hayashi, Saeko S. ; Oasa, Yumiko ; Fukagawa, Misato ; Kaifu, Norio ; Suto, Hiroshi ; Murakawa, Koji ; Doi…

(Citation)
Publications of the Astronomical Society of Japan,54(6):963-967

(Issue Date)
2002-12-25

(Resource Type)
journal article

(Version)
Version of Record

(URL)
https://hdl.handle.net/20.500.14094/90001435

PASJ: Publ. Astron. Soc. Japan **54**, 963–967, 2002 December 25

Near-Infrared Coronagraphy of the GG Tauri A Binary System *

Yoichi ITOH,[1] Motohide TAMURA,[2] Saeko S. HAYASHI,[3] Yumiko OASA,[4]
Misato FUKAGAWA,[5] Norio KAIFU,[2] Hiroshi SUTO,[3] Koji MURAKAWA,[3]
Yoshiyuki DOI,[3] Noboru EBIZUKA,[6] Takahiro NAOI,[5] Hideki TAKAMI,[3]
Naruhisa TAKATO,[3] Wolfgang GAESSLER,[3] Tomio KANZAWA,[3]
Yutaka HAYANO,[2] Yukiko KAMATA,[2] David SAINT-JACQUES,[2]
and
Masanori IYE[2]

[1]*Graduate School of Science and Technology, Kobe University, 1-1 Rokkodai, Nada, Kobe, Hyogo 657-8501*
yitoh@kobe-u.ac.jp
[2]*National Astronomical Observatory, 2-21-1 Osawa, Mitaka, Tokyo 181-8588*
[3]*Subaru Telescope, 650 N. A'ohoku Pl., Hilo, Hawaii 96720, USA*
[4]*National Space Development Agency of Japan, 1-8-10 Harumi, Chuo, Tokyo 104-8023*
[5]*Graduate School of Science, The University of Tokyo, 7-3-1 Hongo, Bunkyo-ku, Tokyo 113-0033*
[6]*The Institute of Physical and Chemical Research, 2-1 Hirosawa, Wako, Saitama 351-0198*

(Received 2002 August 20; accepted 2002 October 10)

Abstract

The highest angular resolution near-infrared images of the GG Tau A binary system were obtained with the Coronagraphic Imager with Adaptive Optics (CIAO) mounted on the Subaru Telescope. The images show that its circumbinary disk is smooth and does not have 0.″1 scale structures. Asymmetries in the surface brightness as well as a gap are also resolved. Combined with previous measurements of the stellar positions, our data indicate that the central binary is unlikely to have a large eccentricity. The fifth point source toward this double binary system is probably a background star, based on astrometric measurements.

Key words: stars: individual (GG Tauri) — stars: pre-main sequence — techniques: high angular resolution

1. Introduction

GG Tau is a well-studied young multiple system. The system has two binaries, GG Tau Aa/Ab and GG Tau Ba/Bb. The GG Tau A binary (hereafter GG Tau) is especially interesting, because it possesses a circumbinary disk which is spatially resolved in the millimeter wavelengths (Kawabe et al. 1993; Guilloteau et al. 1999), in the near-infrared (Roddier et al. 1996; Silber et al. 2000; Potter et al. 2001; McCabe et al. 2002), and recently in the optical (Krist et al. 2002).

The large-scale structure of the circumbinary disk is well characterized by an annulus with an inner radius of 180 AU ($\sim 1.''27$) and a width of 88 AU ($\sim 0.''63$). The disk is inclined by $\sim 37^\circ$ with the northern edge nearest us. The kinematics of the disk are consistent with Keplerian rotation (Guilloteau et al. 1999).

Disk asymmetry and irregularity as well as the presence of small structures associated with the disk have been pointed out, though some of them are controversial. Near-infrared images of Roddier et al. (1996) show a clumpy structure in the disk, whereas near-infrared images taken by HST/NICMOS (Silber et al. 2000) and optical images by HST (Krist et al. 2002) show a smooth structure. The HST observations suggest the presence of a gap in the west portion (Silber et al. 2000; Krist et al. 2002) and a kink at the south-east (Krist et al. 2002; McCabe et al. 2002). Inside the disk, a spoke structure is suggested by Roddier et al. (1996) and Potter et al. (2001), but not confirmed by the HST observations (Silber et al. 2000; Krist et al. 2002). Near-infrared images by Silber et al. (2000) indicate the presence of cavity materials, whereas Krist et al. (2002) suggest an arc structure close to the central binary.

The structure of the circumbinary disk may be affected by the central binary. Computer simulations predict that the binary makes a hole inside the disk (e.g. Artymowicz, Lubow 1994), and that a binary with large eccentricity introduces density-distribution inhomogeneities within the disk (Imaeda 2001). However, the orbital elements of the central binary are also controversial. Roddier et al. (1996) proposed an eccentric orbit in which the stars are located near periastron at the time of the observations, whereas Krist et al. (2002) proposed that the stars are near apoastron in a highly eccentric orbit. Very recently McCabe et al. (2002) derived a slightly elliptical orbit $e = 0.3 \pm 0.2$ with a semi-major axis of $a = 35^{+22}_{-8}$ AU.

We present here near-infrared coronagraphy of the GG Tau system. Combining the coronagraph with the adaptive optics system, we obtained the highest spatial resolution and highest signal-to-noise ratio images of the GG Tau system ever. The observations are described in section 2, and the data-reduction procedures in section 3. In section 4, we discuss the orbital elements of the central binary of GG Tau, the structure of the circumbinary disk around GG Tau, and the nature of the fifth component.

* Based on data collected at Subaru Telescope, which is operated by the National Astronomical Observatory of Japan.

2. Observations

Near-infrared coronagraphic observations were carried out on 2001 January 16 with the Coronagraphic Imager with Adaptive Optics (CIAO, Tamura et al. 2000) on the Subaru Telescope. The observations were carried out as the first light of CIAO in conjunction with the Adaptive Optics (AO) system (Gaessler et al. 2002). CIAO has occulting masks at the first focal plane and Lyot stops at the pupil plane, both of which are selectable and cooled cryogenically. The occulting masks are made of chrome on a sapphire substrate, and have a transmittance of a few tenths of a percent, which enable us to measure the exact position of the central object(s). The mask which we used was $0\farcs8$ in diameter, in order to block light from both components of the binary. We used the traditional circular Lyot stop, whose diameter was 0.8 times as large as the pupil diameter. The 1024×1024 InSb Alladin II array detector was located at the second focal plane. The field of view is $21\farcs96 \times 21\farcs96$ with a spatial scale of $0\farcs02145\,\mathrm{pixel}^{-1}$, using the medium-resolution mode of the camera optics. The pixel scale was measured by observations of the Trapezium cluster (Simon et al. 1999) with the same optical configurations. The uncertainty in the pixel scale was $0\farcs00025\,\mathrm{pixel}^{-1}$ and that in the orientation was $0\fdg073$. The observations were carried out in the H- and K-bands. The typical seeing size was $0\farcs6$. The sky was covered by thin cirrus throughout the observations. The exposure time was 10 s, and we coadded 3 exposures into one frame. The total integration time was 450 s and 540 s for the H- and K-bands, respectively. As discussed later, some frames were rejected during data reduction due to a poor AO correction. As a PSF reference star, SAO 93992 was observed immediately after the observations of GG Tau with the same configurations. Dome flats were taken at the end of the night using an incandescent lamp. Exposures for dark frames were also taken at the end of the night.

3. Data Reduction and Results

The Image Reduction and Analysis Facility (IRAF) software was used for all the data reduction. First, a dark frame was subtracted from the object frame, then the frame was divided by the dome-flat. Hot and bad pixels were removed. Although we carried out observations with the AO, the peak position of the PSF changed slightly during the observations. This was mainly due to the differences in the atmospheric distortion between the infrared wavelengths (at which the images were taken) and the optical wavelengths (at which the wavefront was measured). We measured the peak position of the reference star PSF with the **`imexamine`** Task, and then the images were shifted. Since the Subaru Telescope is an alt–azimuth telescope and we used the instrument rotator, the position angle of the spider changed with time. Therefore, the frames of the reference star were rotated to adjust the position angle of the spider to that of each object frame, and then combined. Next, we measured the relative flux and the peak position of the GG Tau binary with the **`imexamine`** task in each frame. We then created pseudo-binary images; the combined reference image was duplicated, and then shifted to adjust the peak positions of the PSFs between the reference star and each component of the GG Tau binary; the pixel value of the reference image was scaled to adjust the flux ratio between each component of the GG Tau binary, then two reference images were combined into one pseudo-binary image. The pseudo-binary was renormalized to match the wings of the GG Tau image $0\farcs7$ from the center of the system. Then, the scaled pseudo-binary image was subtracted from the object frame. As poor weather condition made the AO correction unstable, first six frames of the H-band object image and twelve frames of the K-band image were rejected. Finally, the object frames were combined.

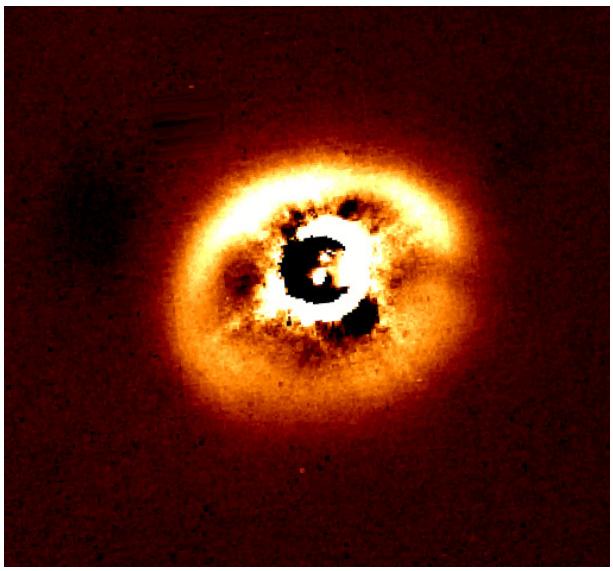

Fig. 1. H-band coronagraphic image of GG Tau. PSFs of the central binary were subtracted. The field of view is $10\farcs16 \times 9\farcs79$. North is up, east toward the left. The effective integration time of this image was 270 s.

The H-band coronagraphic image of the circumbinary disk around GG Tau is presented in figure 1. The central binary was imaged within the occulting mask with a significant suppression of its light. The FWHM of the binary PSF is $0\farcs09$, as derived from a Moffat function fitting. The Strehl ratio was around 0.05. Note that the run was carried out as the second run of the AO system. The current performance has been improved. Because the FWHM of the PSF of the HST/NICMOS observations at 1 μm is about $0\farcs1$ (Silber et al. 2000), figure 1 is the highest spatial-resolution image of GG Tau in the near-infrared wavelengths. The bright portion just around the mask is an artifact, made by residuals in the halo of the object, as well as by the positional discrepancy between the object and the reference star with respect to the mask. Subtraction residuals of diffraction made by the spider are also seen as a cross. Nevertheless, the circumbinary disk is clearly detected. No structure can be found in the circumbinary disk. This fact indicates that there is no clumpy structure in the disk around the $0\farcs1$ (14 AU) scale.

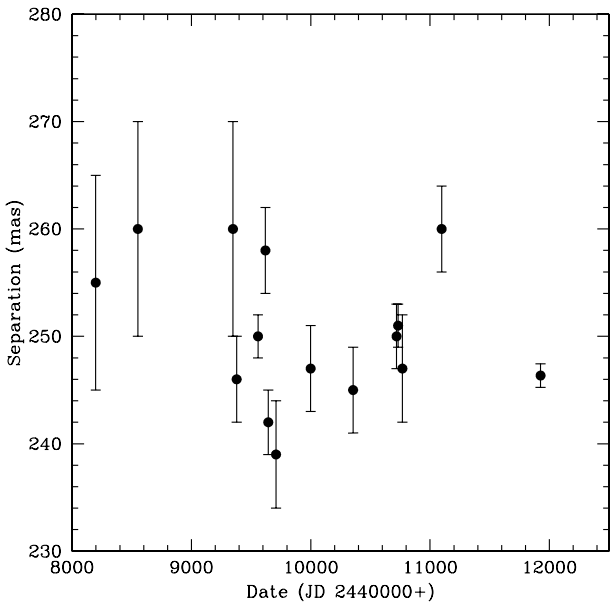

Fig. 2. Time variation of the separations of the central binary. Data were taken from Roddier et al. (1996), Ghez et al. (1995), Silber et al. (2000), Woitas et al. (2001), Krist et al. (2002), McCabe et al. (2002), and this work.

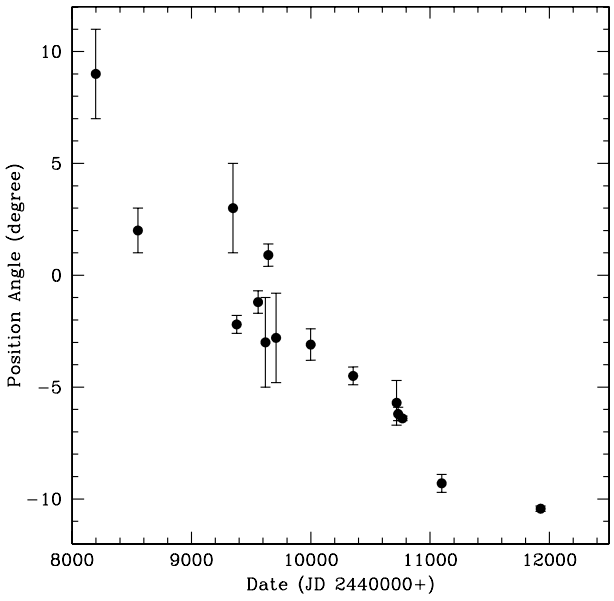

Fig. 3. Time variation of the position angle of the central binary.

4. Discussion

4.1. Binary Component

Astrometric measurements of a binary system give us the orbital elements of the binary. The position of the GG Tau binary was measured during the last ten years (Roddier et al. 1996; Ghez et al. 1995; Silber et al. 2000; Woitas et al. 2001; Krist et al. 2002; McCabe et al. 2002). Because the PSFs of the binary did not saturate when using the occulting mask, we accurately measured the positions of the binary. The separation is 246.4 ± 1.1 mas and the position angle is $-10.^\circ44 \pm 0.^\circ12$. The uncertainties are the standard deviation of the measurements of each frame (0.05 pixel and $0.^\circ09$), and the uncertainty in the pixel scale and in the orientation of the detector. Figures 2 and 3 show the time variations of the separation and the position angle of the binary. The separation of the binary is nearly constant, whereas the position angle changed by 20° during the past ten years. If the orbit of the binary is coplanar to the circumbinary disk, the orbit has an inclination of 37° and a position angle of −7°. A weighted linear fit of the deprojected separation of the binary gives an average of 310 mas, a slope of $-1.03\,\mathrm{mas\,yr^{-1}}$, and a standard deviation (σ) of 8.21 mas. However, because the fitting correlation is poor, we conclude that the deprojected separation had been constant between 305 mas and 315 mas for the past ten years. The fit of the deprojected position angle gives a slope of $-1.^\circ12\,\mathrm{yr^{-1}}$ and a σ of $1.^\circ69$.

We now consider the orbital motion of the secondary object in the rest frame of the primary. The separation r and the position angle f of the binary are given as

$$r = a(1 - e\cos E), \tag{1}$$

$$f = \cos^{-1}\left(\frac{\cos E - e}{1 - e\cos E}\right), \tag{2}$$

$$E = M + 2\sum_{s=1}^{\infty}\frac{1}{s}J_s(se)\sin(sM), \tag{3}$$

$$M = \Omega t, \tag{4}$$

$$\Omega = \sqrt{\frac{Gm}{a^3}}, \tag{5}$$

$$m = m_1 + m_2, \tag{6}$$

where a is the semi-major axis, e is the eccentricity, t is the time, G is the gravitation constant, m_1 and m_2 are the masses of the binary components, and J_s is a Bessel function (Murray, Dermott 1999). The mass of each component of the GG Tau binary is deduced to be $0.78\,M_\odot$ and $0.68\,M_\odot$, respectively (White et al. 1999).

We consider the following two cases for solutions in the orbital elements:

- Case A: Solutions with 1σ precision (68% confidence level):
  the deprojected separation is (305–315) ± 8.21 mas,
  the change of the position angle in ten years is $-11.^\circ21 \pm 1.^\circ68$.
- Case B: Solutions with 2σ precision (95% confidence level):
  the separation is (305–315) ± 16.42 mas,
  the change of the position angle is $-11.^\circ21 \pm 3.^\circ36$.

Figure 4 shows orbital elements consistent with the observational value with 1σ precision (filled squares) and those with 2σ precision (open squares). The orbital elements with semi-major axes less than 45 AU have a solution close to its apoastron, while those with axes greater than 45 AU have one close to its periastron. The orbital elements deduced by McCabe et al. (2002) also have a solution.

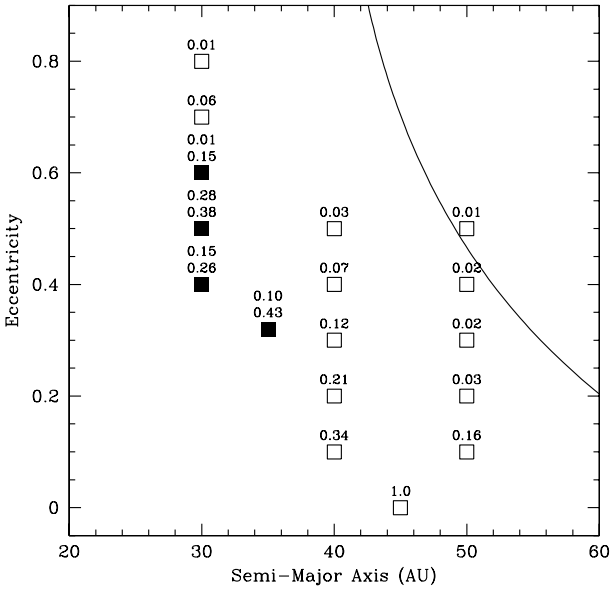

Fig. 4. Orbital elements of the binary. The filled squares show the orbital elements where the position angle and the separation are consistent with the observational values to $1\,\sigma$ precision (of the observational values). The open squares show the orbital elements to $2\,\sigma$ precision. The solid line represents the critical orbital elements. The circumbinary disk is stable if the binary has a lower eccentricity and a smaller semi-major axis than the critical values. The probability that the separation and the position angle are consistent with the observed values in one orbital period is denoted by the number above the squares (upper for $1\,\sigma$ precision and lower for $2\,\sigma$ precision). The orbital elements deduced by McCabe et al. (2002) (a = 35 AU, e = 0.32) have a solution.

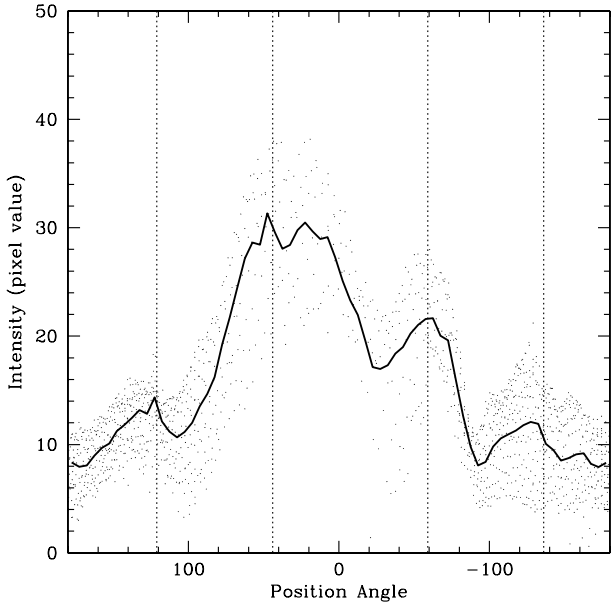

Fig. 5. H-band azimuthal profile intensity of the circumbinary disk. The dots represent the average pixel value of the image in a 3 by 3 pixel aperture. The solid line shows the average of the intensity within 5°. The vertical lines represent the position angles of the spider.

The solid line in figure 4 represents the critical orbital elements of the binary deduced from equation (3) of Holman and Wiegert (1999). These critical parameters are defined as the longevity for a small particle at 180 AU from the centroid of the binary to survive 10^4 orbital periods of the binary. For the GG Tau system, the period corresponds to an order of 10^6 yr. If the binary has a lower eccentricity and a smaller semi-major axis than the critical values, the circumbinary disk with an inner radius of 180 AU is stable. On the other hand, if the binary has either a higher eccentricity or a larger semi-major axis than the critical values, an inner portion of the disk becomes unstable.

The probability that both the separation and the position angle are consistent with the observed values in one orbital period is also denoted in figure 4. The orbit with e = 0.0 has a solution at any position angle, whereas the probability decreases significantly with increasing eccentricity. Therefore, it is unlikely that the binary has an orbit with high eccentricity. Imaeda (2001) found that inhomogeneities in the density distribution are formed in the circumbinary disk if the central binary has a high eccentricity. Millimeter observations of the disk (Guilloteau et al. 1999) revealed that the disk is modeled by a uniform ring model. Therefore, the disk morphology is consistent with the estimate that the binary does not have a high eccentricity.

4.2. *The Circumbinary Disk*

The structure of the circumbinary disk is well described by a smooth annulus with a gap. Figure 5 shows the azimuthal profile of the H-band surface brightness of the disk. As clearly shown, the north portion is brighter than the south. The brightest part in the disk is located at position angles of between 20° and 60°, in agreement with Silber et al. (2000) and Krist et al. (2002). The maximum intensity ratio in the disk is ~ 4.0, consistent with the value of the 1-μm image (Silber et al. 2000), and lower than the value of the I-band image (Krist et al. 2002). The gap detected by Silber et al. (2000), Krist et al. (2002), and Potter et al. (2001) is evident as a sudden dip at P.A. $\sim -92°$ in figure 5. The gap may be made by shadowing by the inner material, such as an unknown dense clump.

Figure 6 shows the distance of the disk from the centroid of the binary weighted by the disk brightness. Evidently, the brightest position is closer in the northern part than in the south, indicating an inclined disk. The solid line in figure 6 represents the brightness-weighted distance for the inclined homogeneous disk model proposed by Guilloteau et al. (1999). The fact that the observed distance is well fitted by the model demonstrates that the disk is homogeneous on a large scale. A discrepancy at $-90°$ is made by the gap, and that around $-130°$ is made by subtraction residuals of the spider. No significant discrepancy occurs at the region identified as a kink (Silber et al. 2000) at P.A. $\sim 130°$. The subtraction residual of the spider diffraction might make it difficult to detect the kink.

No confident evidence has been detected for the spokes (Roddier et al. 1996) or the cavity materials (Silber et al. 2000) inside the disk.

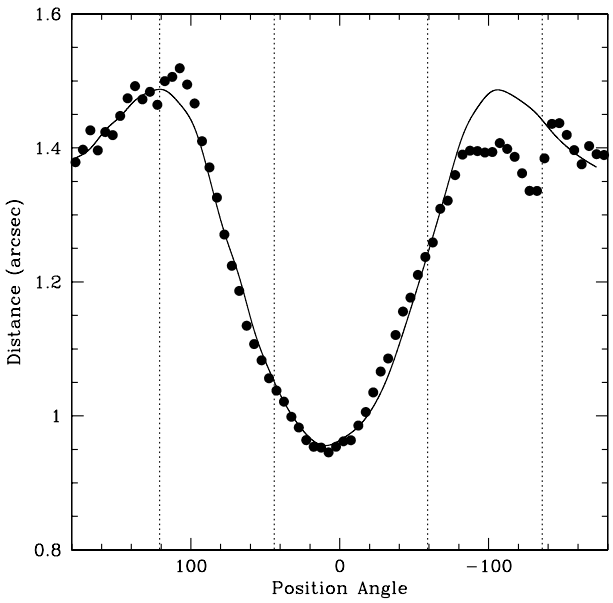

Fig. 6. Brightness-weighted distance of the disk from the centroid of the binary in the H-band. The solid line shows the distance for the inclined homogeneous disk. The vertical lines represent the position angles of the spider.

4.3. Fifth Point Source

We also detected a fifth point source, previously detected by Silber et al. (2000). As the observations were carried out under a cirrus condition, photometry was performed relative to GG Tau Ba (White et al. 1999). The derived magnitudes are 17.15 ± 0.09 and 17.40 ± 0.14 at the H- and K-bands, respectively. If the object is associated with the Taurus molecular cloud, the absolute magnitudes are about 12 mag at both the H- and K-bands. Combining the evolutionary track of Burrows et al. (1997) with the synthetic spectra of Allard et al. (2000), an object of 6 Jupiter mass with an age of 1 Myr old has an absolute magnitude of about 10 mag at both the H- and K-bands. Therefore, the object has a planetary mass. Such objects have been found in other star-forming regions (Oasa et al. 1999).

The object is located $6\farcs123$ from the primary of the GG Tau binary (GG Tau Aa) at a position angle of $242\fdg84$. We calculated the proper motion of the object by comparing the astrometric measurement of the Subaru observations with that of the HST/NICMOS observations (Silber et al. 2000). The separation of the epoch between these observations is about 3 yr. As discussed above, the orbit of the binary is likely to be circular. Given the mass of each component of the binary and assuming the fifth object as a planetary mass object, the centroid of the system was derived. The separation and the position angle between the object and the centroid were $6\farcs209$ and $240\fdg91$ at the time of the NICMOS observations, and $6\farcs160 \pm 0\farcs007$ and $241\fdg74 \pm 0\fdg07$ at the Subaru observations. If the object is associated with the binary, the separation is at least 860 AU, with a corresponding orbital period of more than 2×10^4 yr. Therefore, by assuming a circular orbit, the orbital motion is only $0\fdg05$ in 3 yr, so that the change in the position angle between the HST observations and the Subaru observations is not consistent with the explanation that the object is associated with the binary.

The proper motion of GG Tau is derived to be $(\mu_\alpha, \mu_\delta) = (0\farcs011\,\mathrm{yr}^{-1}, -0\farcs028\,\mathrm{yr}^{-1})$ (Frink et al. 1997). If the fifth object is a distant background star, the separation and position angle would change from $6\farcs209$ and $240\fdg91$ during the HST observations, to $6\farcs198$ and $241\fdg74$ at the time of the Subaru observations. This is consistent with the values derived from the Subaru observations. Therefore, the object is likely to be a background star. The expected number of background stars toward the Taurus molecular cloud is estimated to be 0.22 for the entire field of view of CIAO, or only 0.05 within a $6''$ radius for $H = 17$ (Itoh et al. 1999).

We are grateful to B. Potter for help with the observations. We also thank S. Takahashi and K. Moriwaki for a discussion on the celestial mechanics. Y. I. is supported by the Sumitomo Foundation. Subaru Telescope is operated by the National Astronomical Observatory of Japan.

References

Allard, F., Hauschildt, P. H., & Schweitzer, A. 2000, ApJ, 539, 366
Artymowicz, P., & Lubow, S. H. 1994, ApJ, 421, 651
Burrows, A., Marley, M., Hubbard, W. B., Lunine, J. I., Guillot, T., Saumon, D., Freedman, R., Sudarsky, D., & Sharp, C. 1997, ApJ, 491, 856
Frink, S., Röser, S., Neuhäuser, R., & Sterzik, M. F. 1997, A&A, 325, 613
Gaessler, W., Takami, H., Takato, N., Hayano, Y., Kamata, Y., Saint-Jacques, D., Minowa, Y., & Iye, M. 2002, Proc. SPIE, 4494, 30
Ghez, A. M., Weinberger, A. J., Neugebauer, G., Matthews, K., & McCarthy, D. W., Jr. 1995, AJ, 110, 753
Guilloteau, S., Dutrey, A., & Simon, M. 1999, A&A, 348, 570
Holman, M. J., & Wiegert, P. A. 1999, AJ, 117, 621
Imaeda, Y. 2001, PhD Thesis, The University of Tokyo
Itoh, Y., Tamura, M., & Nakajima, Y. 1999, AJ, 117, 1471
Kawabe, R., Ishiguro, M., Omodaka, T., Kitamura, Y., & Miyama, S. M. 1993, ApJ, 404, L63
Krist, J. E., Stapelfeldt, K. R., & Watson, A. M. 2002, ApJ, 570, 785
McCabe, C., Duchêne, G., & Ghez, A. M. 2002, ApJ, 575, 974
Murray, C. D., & Dermott, S. F. 1999, Solar System Dynamics (Cambridge: Cambridge University Press)
Oasa, Y., Tamura, M., & Sugitani, K. 1999, ApJ, 526, 336
Potter, D., Baudoz, P., Guyon, O., Brandner, W., Close, L., Graves, J. E., & Northcott, M. 2001, BAAS, 33, 812
Roddier, C., Roddier, F., Northcott, M. J., Graves, J. E., & Jim, K. 1996, ApJ, 463, 326
Silber, J., Gledhill, T., Duchêne, G., & Ménard, F. 2000, ApJ, 536, L89
Simon, M., Close, L. M., & Beck, T. L. 1999, AJ, 117, 1375
Tamura, M., Suto, H., Itoh, Y., Ebizuka, N., Doi, Y., Murakawa, K., Hayashi, S. S., Oasa, Y., Takami, H., & Kaifu, N. 2000, Proc. SPIE, 4008, 1153
White, R. J., Ghez, A. M., Reid, I. N., & Schultz, G. 1999, ApJ, 520, 811
Woitas, J., Köhler, R., & Leinert, Ch. 2001, A&A, 369, 249